Beam-Centroid Tracking Instrument for Ion Thrusters

20 March 1995

DTIC
SELECTED
APR 2 6 1995
G

Prepared by

J. E. POLLARD
Mechanics and Materials Technology Center
Technology Operations

Prepared for

SPACE AND MISSILE SYSTEMS CENTER
AIR FORCE MATERIEL COMMAND
2430 E. El Segundo Boulevard
Los Angeles Air Force Base, CA 90245
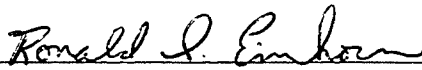
Development Group

19950425 133

THE AEROSPACE CORPORATION
El Segundo, California

R. S. Einhorn, Capt. USAF
SMC/XRI

REPORT DOCUMENTATION PAGE

1. AGENCY USE ONLY (*Leave blank*)	2. REPORT DATE 20 March 1995	3. REPORT TYPE AND DATES COVERED

4. TITLE AND SUBTITLE

Beam-Centroid Tracking Instrument for Ion Thruster

5. FUNDING NUMBERS

F04701-93-C-0094

6. AUTHOR(S)

J. E. Pollard

7. PERFORMING ORGANIZATION NAME(S) AND ADDRESS(ES)

The Aerospace Corporation
Technology Operations
El Segundo, CA 90245-4691

8. PERFORMING ORGANIZATION REPORT NUMBER

TR-94(4507)-1

9. SPONSORING/MONITORING AGENCY NAME(S) AND ADDRESS(ES)

Space and Missile Systems Center
Air Force Materiel Command
2430 E. El Segundo Boulevard
Los Angeles Air Force Base, CA 90245

10. SPONSORING/MONITORING AGENCY REPORT NUMBER

SMC-TR-95-13

11. SUPPLEMENTARY NOTES

12a. DISTRIBUTION/AVAILABILITY STATEMENT

Approved for public release; distribution unlimited

12b. DISTRIBUTION CODE

13. ABSTRACT (*Maximum 200 words*)

Thrust vector stability for an electrostatic ion engine can be measured with improved sensitivity and time resolution by the method described here. Four double-wire Langmuir probes, aligned in the form of a cross, are placed in the exhaust plume and are translated by a motorized positioning system to balance the currents collected along two orthogonal axes. The thrust vector position is thereby measured with an angular resolution of $<0.01°$ and a response time of <5 s.

14. SUBJECT TERMS

Electric propulsion, Xenon ion thruster

15. NUMBER OF PAGES
6

16. PRICE CODE

17. SECURITY CLASSIFICATION OF REPORT UNCLASSIFIED	18. SECURITY CLASSIFICATION OF THIS PAGE UNCLASSIFIED	19. SECURITY CLASSIFICATION OF ABSTRACT UNCLASSIFIED	20. LIMITATION OF ABSTRACT

Contents

Figures

Table

i

I. INTRODUCTION

Spacecraft propulsion based on electrostatic acceleration of ions[1] has a long history of development in the United States,[2,3] the United Kingdom,[4] Germany[5] and Japan.[6] In a typical ion thruster, a plasma discharge is sustained with dc or rf electric and magnetic fields, and a kilovolt ion beam is extracted using closely spaced grid plates perforated with a mesh of holes. A hollow cathode discharge (external to the main plasma) provides electrons for neutralization of the accelerated beam. After the early emphasis on mercury and cesium propellants, xenon was adopted in the 1980s to eliminate possible metallic deposition on spacecraft surfaces, to minimize environmental concerns in ground testing, and to simplify the power processing electronics. The high exhaust velocity of ion thrusters (20–40 km/s) reduces the mass of propellant required for a given orbital maneuver, which can improve the payload capabilities, extend spacecraft maneuvering life, or reduce launch costs. These benefits have led to planned flight applications on Japan's Engineering Test Satellite (ETS-6, 1994 launch) and on the European Space Agency's Advanced Relay and Technology Mission (ARTEMIS, 1996 launch).

Ion thrusters have operating characteristics quite different from those of chemical propulsion systems, and incorporating them into a spacecraft design leads to challenges in regard to the mounting configuration, flight operations, and plume/spacecraft interactions. Thrust vector (TV) drift is a potential area of concern for satellite designs using ion propulsion. Short-term drift occurs during each thruster warm-up period, and long-term drift may result from grid erosion. If left uncorrected, a thrust misalignment generates disturbance torques and can change the satellite's orbit in an undesired manner. Early consideration was given to TV control by electrostatic deflection of beamlets[7] or by translating the ion accelerator grid as on NASA's Applications Technology Satellite (ATS-6, 1974 launch),[8] but electromechanically gimbaling the entire thruster is now the most viable technology. Dual-axis gimbals were included with the mercury ion thrusters on NASA's Space Electric Rocket Test (SERT-II, 1970 launch), although the initial alignment proved to be entirely satisfactory without adjustment.[9] NASA later developed reduced-mass gimbal designs during the Ion Auxiliary Propulsion System (IAPS) and Solar Electric Propulsion

System (SEPS) programs,[2] and a European gimbal is planned for use on the ARTEMIS mission.

Thrust measurement techniques for electric propulsion systems[10] have been developed recently based on a spring restoring force, a pendulum, and a gas-bearing turntable, but these methods yield only the thrust magnitude along a single axis. In addition to thrust magnitude, the TV angular offset and stability must be measured to decide whether on-orbit gimbaling will be needed, and to establish requirements for the gimbal angular range and slew rate. There is one previous example of an instrument for measuring thrust magnitude and direction with a pulsed plasma microthruster using a torsion pivot and rotation stage,[11] but this appears to be less convenient for ion engine TV measurements than the concept to be described here. Tests at Giessen University[5] and at Culham Laboratory[12] have used movable Faraday detectors (either single or multiplexed) to map the spatial distribution of ion flux in the exhaust plume, thereby monitoring the TV motion with a time resolution of a few minutes. Flux maps are essential for understanding the transition of the plume from near-field to far-field behavior and for evaluating the beam divergence, but they contain more information than is usually necessary for evaluating TV offset and stability.

We have devised an apparatus for locating the centroid of the ion beam that achieves better time resolution and is simpler to construct than a multiplexed Faraday detector. As shown in Fig. 1, four double-wire Langmuir probes (labeled north, south, east, west) are aligned in the form of a cross, and are suspended in the thruster plume 150–200 cm downstream of the exit plane. The assembly is translated via a motorized positioning system to balance the currents collected along the north–south and east–west axes. Assuming that the plume is azimuthally symmetric, the balance point occurs when the instrument is aligned with the beam centroid, and the thrust vector can thereby be monitored in real time. The measurements reveal the absolute TV offset from the thruster centerline, the extent of TV drift during warm up, and the dependence of TV position on thrust magnitude. This apparatus also records ion flux averaged over the radial extent of the plume, which is a useful diagnostic technique for routine verification of thruster performance. A beam-centroid tracking instrument could be used to measure the TV offset during acceptance testing of thruster flight packages, which would afford an understanding of the unit-to-
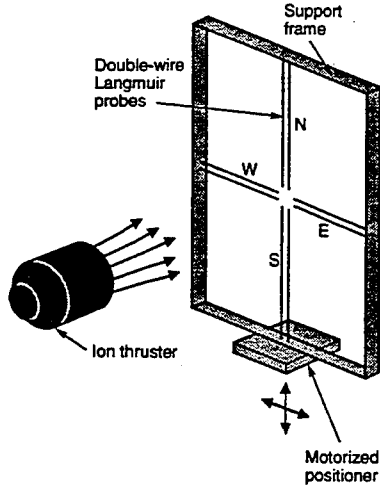
FIG. 1. Four double-wire Langmuir probes are suspended in the far-field plume of an ion thruster, and error signals are generated in proportion to the difference between the two probe currents along the north–south and east–west axes. The motorized positioner moves the assembly to null the error signals, thereby tracking the motion of the beam centroid.

unit variation and would allow for shimming the engine mounts during integration with the spacecraft. The technique described here would also be useful for evaluating TV stability of stationary plasma thrusters, and it could find application in diagnosing broad-beam ion and plasma sources that are widely used for materials processing.[13]

II. APPARATUS DESCRIPTION

A double-wire Langmuir probe[14] consists of two parallel conductors held in close proximity, which are electrically floating with respect to the surrounding plasma and which can be biased relative to each other for measurements of the current as a function of applied voltage. Theoretical considerations in the use of this device to measure ion flux and characteristic electron energy in the plume of a xenon ion thruster have been presented by deBoer.[15] His analysis treats the case of a plasma in which the ions have a directed velocity much greater than their average thermal speed, and in which the electrons have a directed velocity much *less* than their average thermal speed. These conditions are satisfied by a thruster with 1 keV beam energy (40 km/s velocity), having a typical electron thermal speed of $\geqslant 400$ km/s and an ion thermal speed of $\leqslant 4$ km/s. Assuming that the electron distribution is Maxwellian with a temperature T_e, the probe current I as a function of applied voltage V is given by

$$I = n_i u_i eDL(1+\eta)\tanh\left(\frac{eV}{2kT_e}\right). \tag{1}$$

Here the ion density and directed velocity are n_i and u_i, the electronic charge and Boltzmann constant are e and k, the probe wire diameter and length are D and L, and the secondary electron yield is η. Probe current is zero in the absence of an applied voltage, but it approaches a saturation value I_{sat} with increasing voltage, namely
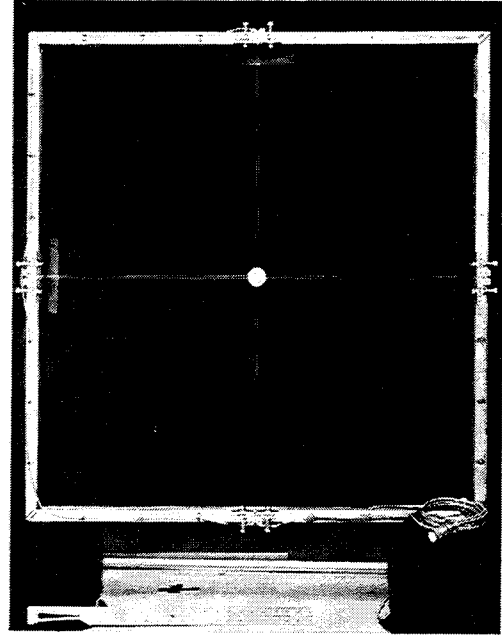

FIG. 2. Photo of the downstream side of the assembly showing probe wires, insulating hub, tensioners, support frame, and multipin connector.

$$|I| \rightarrow I_{sat} \quad \text{for } |eV| \gg 2kT_e,$$

$$I_{sat} \equiv n_i u_i eDL(1+\eta). \tag{2}$$

According to the model, the two wires collect equal numbers of ions from the directed flow regardless of the voltage applied between them. At the asymptotic limit specified in Eq. (2), the negatively biased wire collects no electrons, and the positively biased wire collects a flux of electrons equal to the sum of the ion currents collected by both probe wires. This follows from the assumption that the probe assembly is electrically floating, and hence the net collected current must be zero under steady-state conditions. The foregoing analysis does not account for deflection of the ion trajectories with increasing probe voltage, which causes the two probe wires to collect *different* numbers of ions and thereby show a gradually increasing probe current beyond the voltage at which the probe is "saturated" with respect to the electrons.

As an alternative to the configuration chosen here, it may be feasible to construct a beam-centroid tracking instrument with single-wire probes,[14,15] which are biased several volts negative with respect to the floating potential of the plasma to measure a current proportional to the ion flux. Single-wire probes would permit a slightly simpler mechanical design than the present arrangement, but they have the drawback of perturbing the plasma to a greater extent than with the double-wire configuration.

Probes for this experiment are constructed of various wire materials (0.40-mm-diam Nichrome and 0.81-mm-diam tinned copper have been used successfully) and are supported by a 100 cm×100 cm square frame of welded aluminum channel (see Fig. 2). Each wire is secured at the sup-
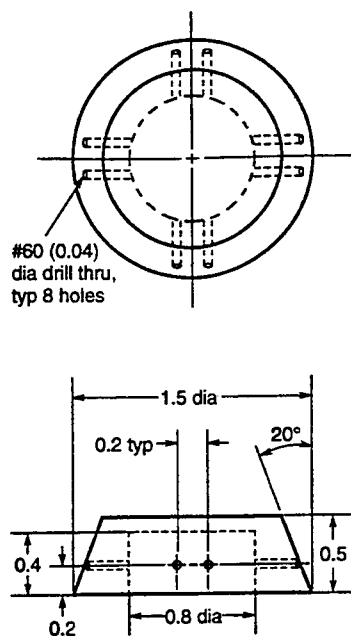
FIG. 3. Machine drawing of the boron nitride hub that holds the probe wires at the center of the assembly (dimensions in inches). Each of the eight wires is inserted through a radial hole and secured on the inside of the hub by bending the wire into a small kink or overhand knot. The upstream face of the hub is tapered by 20° to reduce the buildup of sputtered metal from the wires.

porting frame by a tensioning device that resembles the peg-and-nut mechanism of a violin. The tensioners are shielded from direct beam impingement to avoid spurious currents that would introduce an error in the absolute position of the beam centroid. An insulating hub made of boron nitride (see Fig. 3) holds the probes at the center of the assembly and establishes a wire spacing of 5 mm. During ion bombardment, sputtered metal from the wires is deposited on the insulating hub and eventually can cause an electrical short between the wires. To alleviate this problem the hub is tapered in the upstream direction so that most of the deposits are removed by exposure to the incident ion beam. Each probe has an effective length of $L=42$ cm after accounting for the tensioner shield and insulating hub. When placed 200 cm downstream of the ion accelerator grid, the assembly samples the beam within a 12° half-angle from thruster centerline. Ion flux measurements at Culham Laboratory on a thruster similar to ours have shown that approximately 75% of the total flux is within the solid angle sampled by the probe assembly.[12]

The thruster centerline (i.e., accelerator-grid normal axis) is located by holding a 25-mm-diam mirror against the grid center and observing the backreflection from 4 to 5 m away. Repeated independent trials show that the experimental error in locating this axis is ±0.2°, which is also the estimated uncertainty in the absolute TV position. (This error could be reduced by constructing a custom alignment fixture rather than using a hand-held mirror.) A three-axis motorized

Power supply	Voltage (V)	Current (mA)
Ion beam	1100	453
Main discharge	41.6	3010
Electromagnet	12.7	172
Accelerator grid	−350	2.10
Main hollow cathode	12.6	1000
Neutralizer hollow cathode	19.5	720

positioning system with a resolution of 10 steps/μm (Compumotor 4000) is used for translation of the probe assembly; its coordinate origin is established by aligning the probe axes so as to intersect thruster centerline.

The electrical arrangement uses four digital ammeters (Fluke 45, full scale of 9.9999 mA) and one variable bias supply (HP 6216B) with four of the eight probe wires connected in common (see Fig. 4). Probe signals are carried by shielded multiconductor cables that are routed along the backside of the support frame and from there to a vacuum feedthrough. A laboratory computer reads the four ammeters and commands the positioning system to move by a vertical distance d_v that is proportional to the north/south error signal and by a horizontal distance d_h proportional to the east/west error signal, thereby balancing the currents and tracking the motion of the centroid in real time. Distances are calculated using

$$d_v = G(I_N - I_S)/(I_N + I_S), \tag{3}$$

$$d_h = G(I_E - I_W)/(I_E + I_W), \tag{4}$$

where I_N, I_S, I_E, I_W are the probe currents, and a feedback gain of $G=150$ mm serves to balance the currents rapidly with minimal overshoot. The computer automatically halts the tracking cycles if the current drops below a preset value (i.e., the ion beam turns off) or if the current goes above a preset value (i.e., an electrical short develops between the probe wires). For a typical current of 140 μA per probe, a change in the least significant ammeter digit (±0.1 μA) causes the positioning system to move by ±0.06 mm, which amounts to a TV angular motion of ±0.002°. Each cycle of reading the four currents and moving the probe assembly takes 2.4 s on average.

III. RESULTS AND DISCUSSION

The test article for this work is a two-grid 10-cm-diam xenon ion thruster (engineering-model T5 Mk3) manufactured by the UK Defence Research Agency,[4] which performs as listed in Table I when operated in a vacuum facility at Aerospace Corp. A distinctive feature of the T5 thruster is that the screen grid and accelerator grid are dished inward to prevent a short circuit from occurring due to differential thermal expansion. The resulting convergent trajectories of the ion beamlets produce a beam waist 10–15 cm downstream of the accelerator grid. Background pressure during the test is
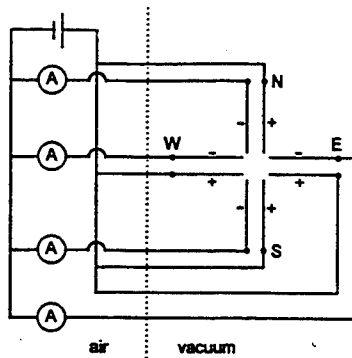
FIG. 4. Electrical schematic showing the four individual probe wires connected to digital ammeters, and the four common probe wires connected to the dc power supply. Positive probe voltage is defined as the four common wires being at a positive potential relative to the four individual wires, as illustrated here. An alternative configuration using four separate dc power supplies with no common probe wires has also been tested.

maintained in the low 10^{-6} Torr range by two re-entrant closed-cycle cryopumps (CVI TM1200) with a combined pumping speed for xenon of 7×10^4 ℓ/s. The beam dump consists of a water-cooled aluminum plate coated with graphite (Aquadag-E) that is located 50–70 cm downstream of the probe assembly.

Langmuir probe current-voltage characteristics are shown in Fig. 5 for operation at a nominal thrust of 19 mN with the probe assembly positioned to equalize the currents at a voltage of +5 V. A positive probe voltage (e.g., +5 V) means that the four *common* wires are positive with respect to the four *individual* wires leading to the ammeters; in this case the individual wires collect only ions at saturation, while the common wires collect both electrons and ions. There is a discrepancy between the curves when the voltage is negative (i.e., when the ammeters are measuring both electrons and ions), but the average of the four currents at negative voltage matches the average at the corresponding positive voltage to within 0.7%. If we assume that high-energy ions in the plume are relatively unaffected by stray electric fields and that all four probes collect equal numbers of ions, the discrepancy means that north, south, east, and west collect unequal numbers of electrons. This is attributed to perturbing electric fields that cause net electron currents to flow between adjacent probes, but we have not been able to establish a detailed mechanism for this process. Rather than the layout shown in Fig. 4, it would seem preferable to minimize the interaction between adjacent probes by hooking up the wires with alternating polarities going around the hub, but the alternating arrangement still gives a discrepancy at negative voltage like that shown in Fig. 5. However, a configuration using four separate power supplies (with no wires connected in common) gives four identical, symmetric current-voltage characteristics, and the measured centroid position is the same as when the standard configuration is operated at positive common probe voltage. Nearly all of the beam centroid data that we have recorded are with the standard configuration at +5 V.
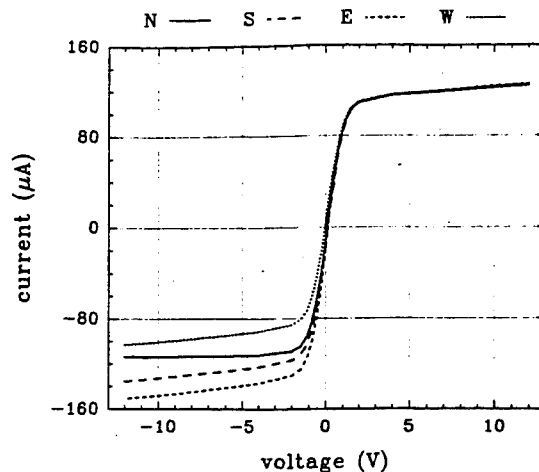

FIG. 5. Langmuir probe current-voltage characteristics when the thruster is operated at 19 mN. The probe assembly is 201 cm from the ion accelerator grid and is positioned to balance the currents at a probe voltage of +5 V. The discrepancy between the four currents at negative voltage is discussed in Sec. III.

Figure 6 shows the average of the four probe currents as a function of voltage. Between −3 and +3 V the data are well represented by the hyperbolic tangent function in Eq. (1), but outside this range the magnitude of the current continues to increase linearly rather than reaching a saturation value. The probable cause is deflection of ion trajectories as mentioned in Sec. II, but there may also be a contribution from increasing secondary electron yield. A least-squares fit to the data in Fig. 6 gives $I_{sat} = 111.5$ μA and $kT_e = 0.47$ eV. The ion flux averaged over the radial extent of the plume at 201 cm from the accelerator grid is then

$$I(\mu A) = 111.5 \tanh(V/0.944) + 1.18 \, V$$
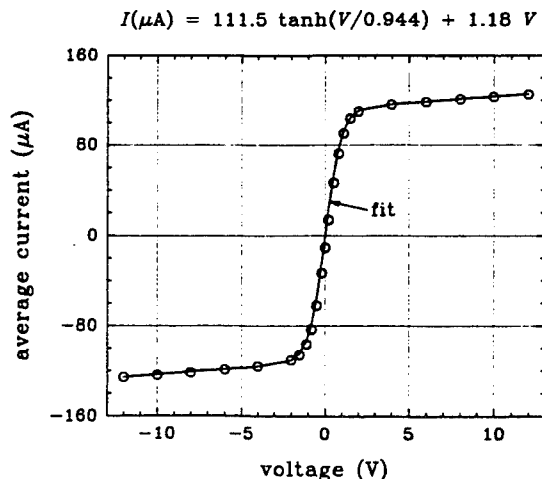

FIG. 6. Current-voltage characteristic averaged over the four probes at 19 mN nominal thrust. Open circles are the measurements, and the solid line is a least-squares fit using Eq. (1) plus a linear term to represent post-saturation behavior (see Sec. II). The average of the four currents at negative voltage matches the average at the corresponding positive voltage to within 0.7%.
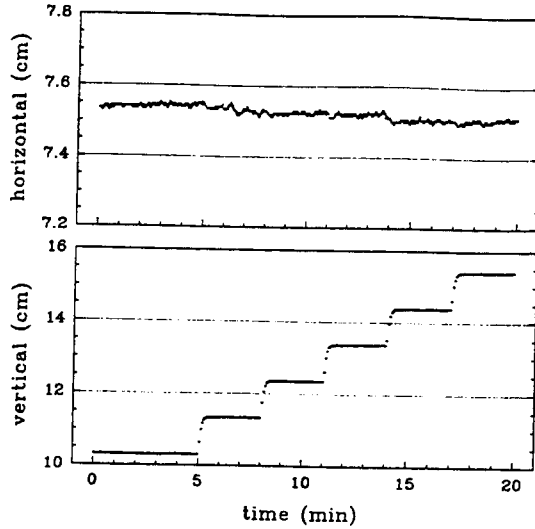
4

FIG. 7. Instrument response as the thruster is translated in 1.02 cm steps by a vertical motion system. Beam-centroid vertical motion matches the thruster motion to within ±1%. Scale for the horizontal axis is magnified by a factor of 10 to show cross coupling.

$$n_i u_i e R^2 = \frac{I_{sat} R^2}{DL(1+\eta)} = \frac{(111.5 \ \mu A)(201 \ cm - 15 \ cm)^2}{(0.040 \ cm)(42 \ cm)(1.04)}$$

$$= 2.2 \ A \, sr^{-1}. \tag{5}$$

Here the ion flux per steradian is calculated with respect to a beam waist located 15 cm downstream of the accelerator grid, and the secondary electron yield is estimated based on data for xenon ions on tungsten.[16] For comparison with the present results, an independent measurement in our facility using smaller movable Langmuir probes has been made at a nominal thrust of 18 mN,[15] which gives a centerline ion flux of 2.3 A sr^{-1} and an average electron energy of $kT_e \approx 0.55$ eV at 60 cm from the accelerator grid.

Relative positional accuracy of the beam-centroid instrument is checked by using a separate translation system to move the thruster vertically in steps of 1.02 cm and observing the motion of the probe assembly (see Fig. 7). The vertical response matches the thruster motion to within ±1%, while the horizontal response (i.e., cross coupling) is 1%–2% of the nominally vertical thruster motion. The settling time at each vertical step corresponds to a maximum instrument slew rate of 2.4 cm/min and a maximum centroid motion of 0.7°/min.

Two possible sources of error in the TV offset are spurious current collected at the edges of the ion beam by the probe-wire tensioners (despite the effort to shield them), and the unmeasured ion flux in the outer regions of the plume. These errors are shown to be minimal by monitoring the apparent centroid position while changing the distance between the thruster and the probe assembly: the centroid moves by less than 0.05° when the distance is varied from 155 to 201 cm. Any errors due to ions scattered from the beam dump are also shown to be negligible by this observation.
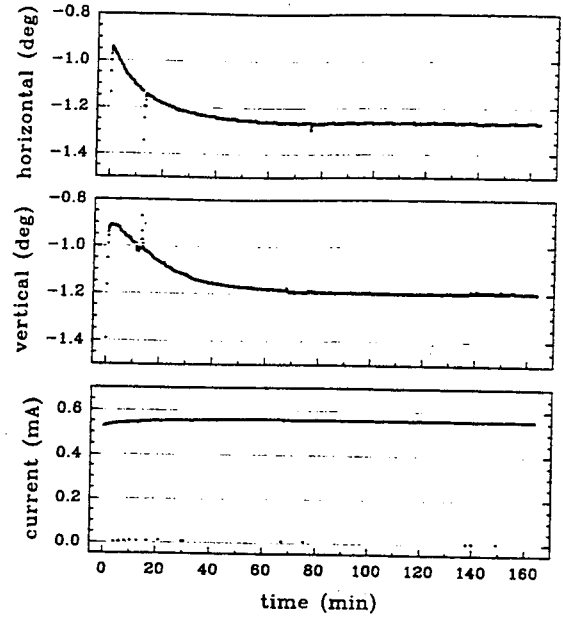

FIG. 8. Thrust vector drift following a cold start at a nominal thrust of 25 mN, with horizontal and vertical deflection given in degrees relative to thruster centerline. The currents are unbalanced for the first five data points while the instrument converges on the centroid position. The lower trace is the summed probe current, which goes to zero several times during this data set when the thruster experiences a momentary grid short followed by a restart.

Because the thin probe wires (<1 mm diam) intercept only a small fraction of the total ion flux, the thrust vector measurement accuracy would be degraded if the plume deviated strongly from azimuthal symmetry. Tests on a similar two-grid T5 thruster at Culham Laboratory using a movable Faraday detector showed that the plume is azimuthally symmetric to within 2%–3%,[12] which justifies the assumption underlying our beam-centroid experiment. Additional confirmation comes from our observation that the north and south currents always agree with the east and west currents to within 2% when the centroid is being tracked.

TV behavior for a cold start at 25 mN is given in Fig. 8, showing a warm-up drift of 0.3° in 40 min, and a steady-state offset from thruster centerline of −1.2° horizontal and −1.2° vertical. (Referring to Fig. 1, the negative horizontal and vertical directions are identified with the west and south axes, respectively.) Prior to a recent realignment of the thruster grids, the offset at 25 mN was −1.3° horizontal and −3.3° vertical, which suggests that TV position is substantially affected by the grid alignment procedure. Independent verification of the absolute offset is obtained from a limited set of beam profile scans made in our facility using a small Langmuir probe and a Faraday detector, which agree with the beam centroid results to within 0.1°. Tests at Culham Laboratory with a movable Faraday detector also showed significant steady-state offsets (0.5° horizontal and 2.4° vertical).[12] Warm-up drift for the device tested here (0.3°) is small enough to be compensated by the spacecraft attitude control system or by thruster gimbaling. However, it may be
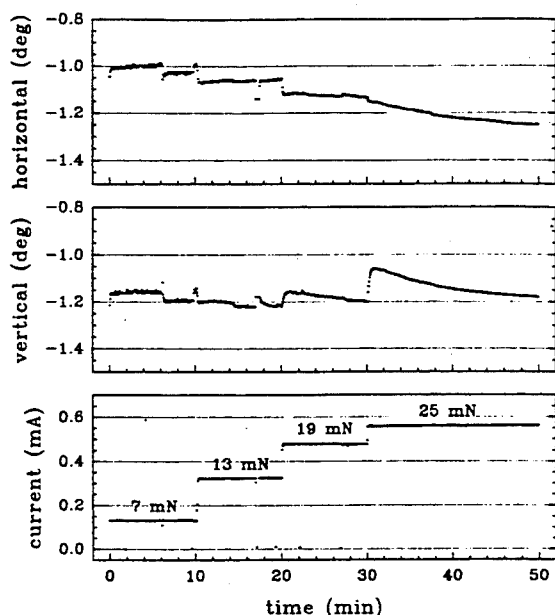
5

FIG. 9. Thrust vector behavior with a fully warmed up engine when the beam current is varied to give nominal thrusts of 7, 13, 19, and 25 mN. The lower trace is the summed probe current, which goes to zero several times during this data set when the thruster experiences a momentary grid short followed by a restart.

possible to save spacecraft cost and mass by eliminating the gimbal, presuming the thruster can be accurately shimmed prior to launch to account for the steady-state offset. Further testing would be required to establish how much the TV has moved after accumulating thousands of operating hours.

The dependence of TV position on thrust level is presented in Fig. 9, showing motions of about 0.2° over the range of 7 to 25 mN. Granularity is evident in the 7 mN data due to the 0.1 μA resolution of the ammeters. Following a change in thrust, the short-term TV displacement is faster than the instrument response, and the longer-term displacement has a time constant of 10–20 min. A valuable adjunct to the centroid measurements is to correlate the TV motion with thruster grid deformations that can be observed using telemicroscopic video cameras.[17] The screen and accelerator grids have different time constants for thermal expansion, and the telemicroscope shows how the gap between the grids changes as a function of discharge power. Differential ther-

mal expansion of the grids is implicated as the primary cause for the observed TV motions.

ACKNOWLEDGMENTS

[1] G. P. Sutton, *Rocket Propulsion Elements*, 6th ed. (Wiley, New York, 1992), pp. 580–590.

[2] V. K. Rawlin, M. J. Patterson, and R. P. Gruber, Proceedings of the 21st International Electric Propulsion Conference, Orlando, FL, 18–20 July 1990 (unpublished), Paper AIAA-90-2527.

[3] J. R. Beattie, J. N. Matossian, and R. R. Robson, J. Propul. Power 6, 145 (1990).

[4] D. G. Fearn, A. R. Martin, and P. Smith, J. Brit. Interplan. Soc. 43, 431 (1990).

[5] K. H. Groh and H. W. Loeb, Rev. Sci. Instrum. 63, 2513 (1992); 65, 1741 (1994).

[6] Y. Arakawa, Proceedings of 23rd International Electric Propulsion Conference, Seattle, WA 13–16 September 1993, (unpublished), Paper IEPC-93-005.

[7] H. J. King and D. E. Schnelker, J. Spacecraft Rockets 8, 552 (1971).

[8] K. E. Clark, J. Spacecraft Rockets 12, 641 (1975).

[9] W. R. Kerslake and L. R. Ignaczak, J. Spacecraft Rockets 30, 258 (1993).

[10] Y. Nakamura and S. Kitamura, Acta Astronautica 7, 1075 (1980); H. Murakami *et al.* J. Spacecraft Rockets 21, 96 (1984); W. E. Morren *et al.* J. Propul. Power 6, 18 (1990); T. W. Haag, Rev. Sci. Instrum. 62, 1186 (1991); A. Sasoh and Y. Arakawa, *ibid.* 64, 719 (1993).

[11] T. E. Williams and R. A. Callens, Proceedings of the 9th Electric Propulsion Conference, Bethesda, MD, 17–19 April 1972 (unpublished), Paper AIAA-72-460.

[12] S. D. Watson *et al.* in Ref. 6, Paper IEPC-93-170.

[13] See for example, H. R. Kaufman and R. S. Robinson, AIAA J. 20, 745 (1982); *Proceedings of the 4th International Conference on Ion Sources* edited by B. H. Wolf [Rev. Sci. Instrum. 63, No. 4, Part II (1992)].

[14] N. Hershkowitz, in *Plasma Diagnostics*, edited by O. Auciello and D. L. Flamm (Academic, San Diego, 1989), Vol. 1, pp. 176–178.

[15] P. C. T. deBoer, in Ref. 6, Paper IEPC-93-236; Aerospace Report No. TR-93(3507)-1, March 1994.

[16] L. B. Loeb, *Basic Processes of Gaseous Electronics*, 2nd ed. (University of California Press, Berkeley, 1960), pp. 764–794, gives data for xenon ions on clean tungsten. Ejection of electrons from metal surfaces by the impact of xenon ions occurs mainly by an Auger-like process, for which the electron yield depends on the charge state of the ion and on the work function and surface coverage of the metal, but the yield is independent of the ion kinetic energy. Our wire materials are expected to have work functions of 4.5–5.0 eV, which are similar to the value of 4.6 eV for clean tungsten. We estimate that the electron yield is about 0.04 for an ion beam containing 10% doubly charged and 90% singly charged xenon.

[17] M. W. Crofton, Proceedings of the 30th Joint Propulsion Conference, Indianapolis, 27–29 June 1994 (unpublished), Paper AIAA-94-2847.

TECHNOLOGY OPERATIONS

The Aerospace Corporation functions as an "architect-engineer" for national security programs, specializing in advanced military space systems. The Corporation's Technology Operations supports the effective and timely development and operation of national security systems through scientific research and the application of advanced technology. Vital to the success of the Corporation is the technical staff's wide-ranging expertise and its ability to stay abreast of new technological developments and program support issues associated with rapidly evolving space systems. Contributing capabilities are provided by these individual Technology Centers:

Electronics Technology Center: Microelectronics, solid-state device physics, VLSI reliability, compound semiconductors, radiation hardening, data storage technologies, infrared detector devices and testing; electro-optics, quantum electronics, solid-state lasers, optical propagation and communications; cw and pulsed chemical laser development, optical resonators, beam control, atmospheric propagation, and laser effects and countermeasures; atomic frequency standards, applied laser spectroscopy, laser chemistry, laser optoelectronics, phase conjugation and coherent imaging, solar cell physics, battery electrochemistry, battery testing and evaluation.

Mechanics and Materials Technology Center: Evaluation and characterization of new materials: metals, alloys, ceramics, polymers and their composites, and new forms of carbon; development and analysis of thin films and deposition techniques; nondestructive evaluation, component failure analysis and reliability; fracture mechanics and stress corrosion; development and evaluation of hardened components; analysis and evaluation of materials at cryogenic and elevated temperatures; launch vehicle and reentry fluid mechanics, heat transfer and flight dynamics; chemical and electric propulsion; spacecraft structural mechanics, spacecraft survivability and vulnerability assessment; contamination, thermal and structural control; high temperature thermomechanics, gas kinetics and radiation; lubrication and surface phenomena.

Space and Environment Technology Center: Magnetospheric, auroral and cosmic ray physics, wave-particle interactions, magnetospheric plasma waves; atmospheric and ionospheric physics, density and composition of the upper atmosphere, remote sensing using atmospheric radiation; solar physics, infrared astronomy, infrared signature analysis; effects of solar activity, magnetic storms and nuclear explosions on the earth's atmosphere, ionosphere and magnetosphere; effects of electromagnetic and particulate radiations on space systems; space instrumentation; propellant chemistry, chemical dynamics, environmental chemistry, trace detection; atmospheric chemical reactions, atmospheric optics, light scattering, state-specific chemical reactions and radiative signatures of missile plumes, and sensor out-of-field-of-view rejection.